Published in final edited form as:
J Neurosci Methods. 2009 February 15; 177(1): 177–182. doi:10.1016/j.jneumeth.2008.10.004.

METHOD DEVELOPMENT AND VALIDATION OF AN IN VITRO MODEL OF THE EFFECTS OF METHYLPHENIDATE ON MEMBRANE-ASSOCIATED SYNAPTIC VESICLES

Trent J. Volz, **Sarah J. Farnsworth**, **Glen R. Hanson**, and **Annette E. Fleckenstein**
Department of Pharmacology and Toxicology, University of Utah, 30 South 2000 East, Room 201, Salt Lake City, UT 84112

Abstract

In vivo methylphenidate (MPD) administration decreases vesicular monoamine transporter-2 (VMAT-2) immunoreactivity in membrane-associated vesicles isolated from the striata of treated rats while concurrently kinetically upregulating VMAT-2-mediated vesicular dopamine (DA) sequestration. The functional consequences of these MPD-induced effects include an increase in both vesicular DA content and exocytotic DA release. This report describes experiments designed to develop and validate an *in vitro* MPD model to further elucidate the molecular mechanism(s) underlying the effects of MPD on the VMAT-2 in membrane-associated vesicles. Method development experiments revealed that *in vitro* MPD incubation of striatal homogenates, but not striatal synaptosomes, increased DA transport velocities and decreased VMAT-2 immunoreactivity in membrane-associated vesicles. An incubation time of 30 min with a MPD concentration of 10 mM was optimal. Method validation experiments indicated that *in vitro* MPD incubation kinetically upregulated VMAT-2 in membrane-associated vesicles, increased vesicular DA content, and increased exocytotic DA release. These results reveal that the *in vitro* MPD incubation model successfully reproduced the salient features of *in vivo* MPD administration. This *in vitro* MPD incubation model may provide novel insights into the receptor-mediated mechanism(s) of action of *in vivo* MPD in the striatum as well as the physiological regulation of vesicular DA sequestration and synaptic transmission. Accordingly, this *in vitro* model may help to advance the treatment of disorders involving abnormal DA disposition including Parkinson's disease, attention-deficit hyperactivity disorder, and substance abuse.

Keywords

dopamine; in vitro; methylphenidate; rotating disk electrode voltammetry; vesicular monoamine transporter-2

1. INTRODUCTION

Methylphenidate (MPD) is a ritalinic acid psychostimulant used to treat attention-deficit hyperactivity disorder and narcolepsy. In the brain, MPD inhibits the clearance of dopamine (DA) from the synaptic cleft by binding to and inhibiting the plasmalemmal DA transporter (DAT) (Volz et al., 2005; Volz and Schenk, 2005; Wayment et al., 1999). MPD also indirectly affects the transport of DA by the vesicular monoamine transporter-2 (VMAT-2); a protein that sequesters cytoplasmic DA inside the synaptic vesicles of nerve terminals. VMAT-2-

Corresponding author: Annette E. Fleckenstein, Ph.D., Department of Pharmacology and Toxicology, University of Utah, 30 South 2000 East, Room 201, Salt Lake City, UT 84112, Phone (801) 585-7474, FAX (801) 585-5111, e-mail fleckenstein@hsc.utah.edu.

containing vesicles may be categorized as either cytoplasmic vesicles or membrane-associated vesicles depending on whether they co-fractionate with striatal synaptosomal membranes after osmotic lysis (Volz et al., 2007). The important and largely undescribed population of membrane-associated vesicles has unique sigmoidal (i.e., cooperative) DA transport kinetics and has the ability to sequester 5–9 fold more DA than cytoplasmic vesicles thereby enabling the membrane-associated vesicles to potentially function as a "DA sink" and prevent cytoplasmic DA concentrations from rising to neurotoxic levels (Volz et al., 2007).

In vivo studies in rats show that a single MPD administration traffics VMAT-2, and presumably associated vesicles, away from synaptosomal membranes into the cytoplasm and thus decreases VMAT-2 immunoreactivity in the membrane-associated vesicle fraction (Sandoval et al., 2002; Volz et al., 2007). Unexpectedly, MPD also kinetically upregulates DA transport into vesicles remaining in the membrane-associated fraction after MPD-induced trafficking (i.e., these vesicles sequester a larger quantity of DA due to a MPD-induced increase in the rate at which the VMAT-2 transports DA) (Volz et al., 2007). The functional consequences of this increase in DA transport are that MPD redistributes DA within nerve terminals from the cytoplasm and into vesicles which in turn increases vesicular DA content and ultimately increases exocytotic DA release (Volz et al., 2007).

Several *in vivo* studies have revealed that D2 receptor activation mediates the MPD-induced vesicle trafficking, kinetic upregulation, and increase in vesicular DA content, while both D2 and muscarinic receptor activation mediate the MPD-induced increase in exocytotic DA release (Sandoval et al., 2002; Truong et al., 2004; Volz et al., 2008). However, additional studies have been hampered by lack of an *in vitro* model system that would allow further study while avoiding generalized (e.g., systemic) toxicity. Additionally, using an *in vitro* platform would permit assessments where the test agent is available only in limited quantities. Such *in vitro* model systems have successfully been developed to study the effects of methamphetamine on the DAT in striatal synaptosomes (Kim et al., 2000; Sandoval et al., 2001). Another model system has been developed to study the effects of *in vitro* MPD applied directly to cytoplasmic vesicles (Easton et al., 2007).

The present report describes experiments designed to develop and validate an *in vitro* MPD model useful for extending the *in vivo* studies described above and to further elucidate the molecular mechanism(s) underlying the effects of MPD on membrane-associated vesicles. The salient features of *in vivo* MPD administration that were reproduced *in vitro* included: 1) trafficking of vesicles away from the membrane-associated vesicle fraction, 2) cooperativity and kinetic upregulation of DA transport into the remaining membrane-associated vesicles, 3) increased vesicular DA content, and 4) increased exocytotic DA release. This *in vitro* model may provide novel insights into the receptor-mediated mechanism(s) of action of MPD in the striatum as well as the physiological regulation of vesicular DA sequestration and synaptic transmission.

2. MATERIALS AND METHODS

2.1. Solutions and Chemicals

Solutions were made using university-supplied deionized water that was further purified to 18 MΩ with a DIamond Water Purification System from Barnstead (Dubuque, IA). The pH 7.4 sucrose buffer contained 320 mM sucrose, 3.8 mM NaH_2PO_4, and 12.7 mM Na_2HPO_4. The pH 7.5 VMAT-2 assay buffer consisted of 25 mM HEPES, 100 mM potassium tartrate, 0.05 mM EGTA, 0.1 mM EDTA, and 2 mM ATP-Mg^{+2}. The pH 7.4 DAT assay buffer consisted of 126 mM NaCl, 4.8 mM KCl, 1.3 mM $CaCl_2$, 16 mM sodium phosphate, 1.4 mM $MgSO_4$, and 11 mM dextrose. The pH 2.5 tissue buffer consisted of 50 mM sodium phosphate, 30 mM citric acid, and 10 % (v/v) methanol. (±)-MPD hydrochloride was supplied by the Research

Triangle Institute (Research Triangle Park, NC). Potassium tartrate was purchased from Fisher Scientific (Fair Lawn, NJ). Sucrose and NaH_2PO_4 were purchased from JT Baker Chemical Company (Phillipsburg, NJ). HEPES, $MgSO_4$, DA hydrochloride, Na_2HPO_4, EGTA, EDTA, NaCl, KCl, $CaCl_2$, sodium phosphate, sodium octyl sulfate, $MgSO_4$, dextrose, citric acid, methanol, and ATP-Mg^{+2} were purchased from Sigma (St. Louis, MO).

2.2. Animals

Male Sprague-Dawley rats (300 – 360 g) were purchased from Charles River Laboratories (Raleigh, NC) and housed in a light- and temperature-controlled room with free access to food and water. All animal procedures were approved by the University of Utah Institutional Animal Care and Use Committee and were conducted in accordance with the National Institutes of Health Guidelines for the Care and Use of Laboratory Animals.

2.3. In vitro incubation

Untreated rats were sacrificed by decapitation and the striata were removed. For synaptic vesicle experiments, each sample consisted of both striata from a rat that were homogenized in 2 ml of ice-cold sucrose buffer containing various concentrations of MPD as described in the figure legends. For K^+-stimulated DA release experiments, each sample consisted of one striata from a rat that was homogenized in 2 ml of ice-cold DAT assay buffer containing MPD as described in the figure legends. The resulting striatal homogenates were incubated for various times (again as described in the figure legends) at 37 °C. The homogenates were then "washed" by centrifugation (22,000 × *g* for 15 min at 4 °C) and the resulting pellet was resuspended in either 2 ml of fresh sucrose buffer (for isolation of synaptic vesicles) containing no MPD or in 500 µl of DAT assay buffer (for K^+-stimulated DA release experiments) which contained no MPD. A similar washing procedure has been used as part of an *in vitro* methamphetamine model (Sandoval et al., 2001).

There were two exceptions to the above *in vitro* incubation procedure. In one experiment (see Fig. 1), striatal synaptosomes were prepared by centrifuging the striatal homogenates at 800 × *g* for 12 min at 4 °C (Volz et al., 2007). The resulting supernatant was then centrifuged at 22,000 × *g* for 15 min at 4 °C to isolate a synaptosomal pellet which was resuspended in 2 ml of fresh sucrose buffer (containing MPD as described in the figure legends), incubated, and washed. In the other exception (see Fig. 2), some striatal homogenates were incubated with MPD for "0" min. In this case the homogenates were prepared with ice-cold MPD-containing sucrose as above and then immediately washed with no intervening 37 °C incubation.

2.4. Synaptic vesicle isolation

After *in vitro* incubation and resuspension in 2 ml of fresh sucrose buffer (see section 2.3.), samples for use in synaptic vesicle experiments were subjected to a centrifugation protocol in order to isolate the cytoplasmic and membrane-associated vesicles as described previously (Volz et al., 2007; Volz et al., 2008). Each sample was centrifuged (800 × *g* for 12 min at 4 °C) to remove nuclear debris. The resulting supernatant was centrifuged (22,000 × *g* for 15 min at 4 °C) to obtain a synaptosomal pellet. The synaptosomal pellet was then resuspended and homogenized in ice-cold water to lyse the synaptosomal membranes. Ice-cold (pH 7.5) 25 mM HEPES and 100 mM potassium tartrate were then added to the synaptosomal pellet homogenate and the resulting mixture was centrifuged (20,000 × *g* for 20 min at 4 °C) to form a membrane-associated vesicle pellet and a supernatant. To isolate cytoplasmic vesicles for use in DA content measurements, 1 mM ice-cold (pH 7.5) $MgSO_4$ was added to the supernatant and the resulting mixture was centrifuged (100,000 × *g* for 45 min at 4 °C) to obtain the cytoplasmic vesicle pellet.

2.5. Measurement of DA Transport Velocities into Membrane-Associated Vesicles

Rotating disk electrode (RDE) voltammetry (Schenk et al., 2005; Volz et al., 2006) was used to measure the initial velocities of inwardly directed vesicular DA transport into membrane-associated vesicles as described previously (Volz et al., 2007; Volz et al., 2008). The membrane-associated vesicle pellet (see section 2.4.) was resuspended in 500 µl of VMAT-2 assay buffer and placed in a cylindrical glass chamber (10 mm internal diameter with a height of 20 mm) maintained at 37 °C by a VWR International (West Chester, PA) Model 1104 Heating Recirculator. A Pine Instruments, Inc. (Grove City, PA) AFMD03GC glassy carbon electrode (5 mm total diameter with a 3 mm diameter glassy carbon electrode shrouded in Teflon) attached to a Pine Instruments MSRX high-precision rotator was lowered into the glass chamber and rotated at 2000 rpm. A Bioanalytical Systems (West Lafayette, IN) LC3D (Petite Ampere) potentiostat was used to apply a potential of +450 mV relative to a Ag/AgCl reference electrode and a detection current baseline was obtained in approximately 5 min. Then, 10.2 µl of an aqueous DA solution was injected using a Hamilton (Reno, NV) CR-700-20 constant rate syringe which resulted in 1.5 µM DA inside the chamber. The current outputs were recorded onto a Tektronix (Beaverton, OR) TDS 1002 digital storage oscilloscope and the initial velocities of DA transport were calculated from the linear slope of the initial apparent zero-order portion of a plot of DA concentration versus time as described previously (Earles et al., 1998; Volz et al., 2006).

The only exception to this was an experiment designed to study the kinetics of DA transport into membrane-associated vesicles (see Fig. 4). In this experiment the applied DA concentrations ranged from 200 nM - 4 µM and the vesicular DA transport velocities were fit to the Hill equation

$$v=(V_{max} \times [DA]^h)/(K_{0.5}{}^h+[DA]^h) \quad \text{(Eq. 1)}$$

with non-linear regression using GraphPad Prism V4.0 (San Diego, CA) as previously described (Motulsky and Christopoulos, 2003;Segel, 1993;Volz et al., 2007). In this equation v is the transport velocity, V_{max} is the maximal transport velocity, [DA] is the initial extravesicular concentration of exogenously added DA, $K_{0.5}$ is formally defined as the substrate concentration at half maximal transport velocity in a sigmoidal response curve, and h is the Hill coefficient. Protein concentrations were measured using a BioRad Laboratories (Hercules, CA) Bradford protein assay.

2.6. VMAT-2 Immunoreactivity

After RDE measurement of DA transport velocities (see section 2.5.), sodium dodecyl sulfate-polyacrylamide gel electrophoresis and western blot analysis were performed on the membrane-associated vesicle samples as previously described (Riddle et al., 2002; Volz et al., 2007). Equal amounts of protein (40 µg of protein as determined by a BioRad Laboratories (Hercules, CA) Bradford protein assay) from each membrane-associated vesicle sample were loaded onto the gel. Bound VMAT-2 antibody was visualized with horseradish peroxidase-conjugated secondary antibody (rabbit secondary from Biosource (Camarillo, CA)) and bands on blots were quantified by densitometry using a FluorChem SP Imaging System from Alpha Inotech Corp. (San Leandro, CA). VMAT-2 antibody was purchased from Chemicon (Temecula, CA).

2.7. Vesicular DA Content

Vesicular DA content was measured by high performance liquid chromatography as described previously (Volz et al., 2007; Volz et al., 2008). The membrane-associated vesicle and cytoplasmic vesicle pellets were prepared as described above (see section 2.4.) and resuspended

in ice-cold tissue buffer at 50 and 100 mg original striatal wet weight/ml of tissue buffer, respectively. The resuspended vesicle preparations were then sonicated for ~10 s and centrifuged (22,000 × *g* for 15 min at 4 °C). A 100 μsl aliquot of the resulting supernatant was injected onto a high performance liquid chromatograph system (4.6 mm × 250 mm Whatman International, Ltd. (Maidstone, England) Partisphere C18 column) that was coupled to an electrochemical detector (+ 730 mV relative to a Ag/AgCl reference electrode). The pH 2.86 mobile phase consisted of 50 mM sodium phosphate, 30 mM citric acid, 0.16 mM EDTA, 1.5 mM sodium octyl sulfate, and 10 % (v/v) methanol (Chapin et al., 1986).

2.8. Measurement of K^+-stimulated DA Release

RDE voltammetry (Schenk et al., 2005; Volz et al., 2006) was used to measure K^+-stimulated DA release in striatal homogenates as previously described (McElvain and Schenk, 1992; Volz et al., 2007). After *in vitro* incubation and resuspension in 500 μl of fresh DAT assay buffer (see section 2.3.), samples were placed in the RDE and a detection current baseline was obtained as described above (see section 2.5.). A small quantity of DAT assay buffer containing an elevated KCl concentration (resulting in 40 mM K^+ inside the RDE glass chamber) was added to the sample to stimulate DA release. The initial velocity of K^+-stimulated DA release (obtained from the first 3 s of release), the magnitude of K^+-stimulated DA release (taken as the maximum amount of DA released), and the duration of K^+-stimulated DA release (the time required for the maximum amount of DA to be released) were calculated and normalized to striatal wet weight as described previously (McElvain and Schenk, 1992; Volz et al., 2007).

3. RESULTS

Initial experiments were conducted to determine whether striatal homogenates or striatal synaptosomes would be affected by *in vitro* MPD incubation. As shown in Fig. 1, *in vitro* MPD incubation of striatal homogenates increased DA transport velocities and decreased VMAT-2 immunoreactivity in membrane-associated vesicles. However, *in vitro* incubation of striatal synaptosomes with MPD had no effect on either transport velocities or immunoreactivity. Striatal homogenates were thus used for all subsequent experiments.

Experiments were then conducted to establish the optimum incubation time. Fig. 2 shows that *in vitro* MPD incubation of striatal homogenates for times of 15, 30, or 45 min all increased DA transport velocities and decreased VMAT-2 immunoreactivity to a similar extent in membrane-associated vesicles. Incubation of striatal homogenates with MPD for “0” min (see Section 2.3. for details) was without effect. An incubation time of 30 min chosen as experimentally convenient and was used for all subsequent experiments.

The minimum concentration of MPD required to affect velocities and immunoreactivity was then determined. *In vitro* incubation of striatal homogenates for 30 min at 37 °C with MPD concentrations of 10, 30, and 60 mM all increased DA transport velocities and decreased VMAT-2 immunoreactivity to a similar extent in membrane-associated vesicles (Fig. 3). Incubation of striatal homogenates with 1 and 5 mM MPD had no effect on velocities or immunoreactivity. A MPD concentration of 10 mM was the lowest that would affect velocities and immunoreactivity and was thus used for all subsequent experiments.

The results presented in Fig. 4 examined the kinetics of vesicular DA transport in membrane-associated vesicles after *in vitro* MPD incubation using the method developed above. The relationship between the initial concentrations of DA and the measured DA transport velocities in membrane-associated vesicles from both control- and MPD-treated samples was sigmoidal, suggesting cooperativity. The velocities depicted in Fig. 4 were modeled by the Hill equation (Eq. 1) and the Hill coefficients were similar from both control- and MPD-treated samples (3.5 ± 0.8 control vs. 4.2 ± 0.5 MPD). MPD increased DA transport in the membrane-associated

vesicles by increasing the V_{max} (0.83 ± 0.07 control vs. 1.61 ± 0.05 fmol/(s × μg protein) MPD, $p < 0.05$). MPD did not change the concentration of DA needed to attain half maximal velocity (designated $K_{0.5}$ to distinguish it from the K_m of Michaelis-Menten kinetics (Motulsky and Christopoulos, 2003;Segel, 1993;Volz et al., 2007); 1.8 ± 0.2 control vs. 1.62 ± 0.05 μM MPD).

Consistent with the increased DA transport velocities shown in Fig. 4, the results presented in Fig. 5 demonstrate that *in vitro* MPD incubation increased DA content in both the cytoplasmic and membrane-associated vesicles. *In vitro* MPD incubation also increased both the magnitude and velocity of K^+-stimulated DA release as well (Fig. 6). However, MPD did not affect the duration of K^+-stimulated DA release (6.6 ± 0.7 vs. 6.3 ± 0.3 s for control vs. MPD, respectively (N =4)).

4. DISCUSSION

4.1. In Vitro Method Development

The first series of experiments in this paper were designed to develop an *in vitro* MPD incubation method that increases DA transport into, and decreases the VMAT-2 immunoreactivity of, membrane-associated vesicles as is seen with *in vivo* MPD administration. The experiments were intended to investigate whether striatal synaptosomes and/or striatal homogenates could be used, as well as to determine the optimal MPD concentration and incubation time. In the first experiment, *in vitro* MPD incubation of striatal homogenates increased DA transport velocities and decreased VMAT-2 immunoreactivity in membrane-associated vesicles while incubation of striatal synaptosomes was without affect (Fig. 1). Striatal homogenates were thus used for all subsequent experiments.

The lack of effect with synaptosomes was unexpected because *in vitro* incubation of striatal synaptosomes has successfully been used to model the effects of methamphetamine on the plasmalemmal DAT (Kim et al., 2000; Sandoval et al., 2001). This suggests that the *in vitro* effects of MPD require some factor that is present in striatal homogenates but is not retained in the preparation of striatal synaptosomes and points to differences in the *in vitro* mechanisms of action of MPD and methamphetamine.

Experiments were then conducted to determine the optimum incubation time of striatal homogenates. *In vitro* MPD incubation for times of 15, 30, or 45 min all similarly increased DA transport velocities and decreased VMAT-2 immunoreactivity in membrane-associated vesicles (Fig. 2). A time of 30 min was chosen for these studies due to experimental convenience. A 30 min incubation time has also been used in an *in vitro* methamphetamine model (Sandoval et al., 2001).

Incubating the striatal homogenates with MPD for “0” min and omitting the 37 °C incubation (i.e., preparing the striatal homogenates in ice-cold sucrose and then immediately washing with no intervening 37 °C incubation as described in section Section 2.3.) did not affect DA transport velocities or VMAT-2 immunoreactivity in membrane associated vesicles (Fig. 2). This suggests that the 37 °C incubation step is necessary to observe the *in vitro* MPD effects. A 37 °C incubation step was also necessary to model the effects of methamphetamine on the plasmalemmal DAT (Sandoval et al., 2001).

The final experiment to establish the method was designed to determine the minimum *in vitro* concentration of MPD that would reproduce the increase in DA transport velocities and decrease VMAT-2 immunoreactivity in membrane-associated vesicles caused by *in vivo* administration of 2 mg/kg or 40 mg/kg, i.p., of MPD (Riddle et al., 2007; Volz et al., 2007; Volz et al., 2008). A MPD concentration of 10 mM was the lowest that would increase DA

transport velocities and decrease VMAT-2 immunoreactivity in membrane-associated vesicles (Fig. 3). This concentration was thus used for all subsequent experiments.

Drug concentrations used *in vitro* can often be several fold different than those achieved *in vivo*. In rats, MPD doses of 9 mg/kg and 20 mg/kg, i.p., (i.e., doses within the 2 mg/kg and 40 mg/kg, i.p., range used to investigate the *in vivo* effects of MPD on membrane-associated vesicles (Riddle et al., 2007; Volz et al., 2007; Volz et al., 2008)) result in MPD concentrations in the brain of 3.13 μg/g and 18.0 μg/g, respectively, 30 min after administration (Patrick et al., 1984; Thai et al., 1999). These brain concentrations equate to approximately 14 μM and 80 μM MPD, assuming a brain density of 1.04 g/ml (Bretz et al., 1974; Lescot et al., 2008; Sabatini et al., 1991). The lowest effective *in vitro* MPD concentration (10 mM) is thus higher than the MPD concentrations achieved in rat brain (14 μM and 80 μM) after *in vivo* administration. However, it should be noted that, while higher than *in vivo* brain concentrations, the 10 mM MPD *in vitro* concentration successfully replicated all the salient effects of *in vivo* MPD administration as discussed in the next section. Additionally, *in vitro* MPD concentrations in the mM range have been used previously to study the effects of MPD on rat brain suspensions (Lackington and Orrego, 1986).

4.2. In Vitro Method Validation

The second series of experiments in this paper was designed to validate the *in vitro* MPD incubation method developed above. The experiments were intended to investigate the effects of *in vitro* MPD incubation on the kinetics of DA transport into membrane-associated vesicles and to determine whether vesicular DA content and DA release are both increased as is seen with *in vivo* MPD administration. In the kinetic analysis experiment, the initial velocity vs. DA concentration curves for membrane-associated vesicles from both control- and MPD-treated groups were sigmoidal shape and were modeled by the Hill equation (Fig. 4). This is inconsistent with Michaelis-Menten kinetics (Fersht, 1998;Segel, 1993) and suggests that the membrane-associated vesicles have positive cooperativity with respect to DA transport. Both a sigmoidal curve and positive cooperativity are also caused by *in vivo* MPD administration (Volz et al., 2007). *In vitro* MPD incubation increased DA transport velocities by increasing the V_{max} of DA transport (Fig. 4) as does *in vivo* MPD administration (Volz et al., 2007). Additionally, the values of $K_{0.5}$ and V_{max}, as well as the Hill coefficients, from control- and MPD-treated *in vitro* groups were similar to those from saline- and MPD-treated animals given *in vivo* MPD administration. *In vitro* MPD incubation thus replicates the salient effects of *in vivo* MPD administration on the kinetics of DA transport into membrane-associated vesicles.

In addition to increasing DA transport velocities, *in vitro* MPD incubation also increased vesicular DA content (Fig. 5). Consistent with this increase in vesicular DA content, *in vitro* MPD incubation increased both the magnitude and velocity of K^+-stimulated DA release (Fig. 6). *In vitro* MPD incubation thus replicated the increases in vesicular DA content and K^+-stimulated DA release seen with *in vivo* MPD administration.

4.3. Conclusion

The *in vitro* MPD incubation model developed and validated in this report successfully reproduced the salient features of *in vivo* MPD administration including: 1) the trafficking of vesicles away from the membrane-associated vesicle fraction, 2) the cooperativity and kinetic upregulation of DA transport into the remaining membrane-associated vesicles, 3) increased vesicular DA content, and 4) increased exocytotic DA release. This *in vitro* MPD incubation model may provide novel insights into the receptor-mediated mechanism(s) of action of *in vivo* MPD in the striatum as well as the physiological regulation of vesicular DA sequestration and synaptic transmission. It also has the potential to be adapted to other compounds or disease models, thus increasing the applicability of the method. Accordingly, this model may help to

advance the treatment of disorders involving abnormal DA disposition including Parkinson's disease, attention-deficit hyperactivity disorder, and substance abuse.

Acknowledgments

This work was supported by grants DA 00869, DA 04222, DA 13367, DA 11389, DA 019447, and DA 00378 from the National Institute on Drug Abuse.

REFERENCES

Bretz U, Baggiolini M, Hauser R, Hodel C. Resolution of three distinct populations of nerve endings from rat brain homogenates by zonal isopycnic centrifugation. J Cell Biol 1974;61:466–480. [PubMed: 4363959]

Chapin DS, Lookingland KJ, Moore KE. Effects of lc mobile phase composition on retention times for biogenic amines, and their precursors and metabolites. Current Separations 1986;7:68–70.

Earles C, Wayment H, Green M, Schenk JO. Resolution of biogenic amine transporter kinetics by rotating disk electrode voltammetry: methodology and mechanistic interpretations. Methods Enzymol 1998;296:660–675. [PubMed: 9779481]

Easton N, Steward C, Marshall F, Fone K, Marsden C. Effects of amphetamine isomers, methylphenidate and atomoxetine on synaptosomal and synaptic vesicle accumulation and release of dopamine and noradrenaline in vitro in the rat brain. Neuropharmacology 2007;52:405–414. [PubMed: 17020775]

Fersht, A. Structure and Mechanism in Protein Science: A Guide to Enzyme Catalysis and Protein Folding. New York: W. H. Freeman and Company; 1998.

Kim S, Westphalen R, Callahan B, Hatzidimitriou G, Yuan J, Ricaurte GA. Toward development of an in vitro model of methamphetamine-induced dopamine nerve terminal toxicity. J. Pharmacol. Exp. Ther 2000;293:625–633. [PubMed: 10773037]

Lackington I, Orrego F. Continuous measurement of net potassium movements in rat brain cortex suspensions. Effects of glutamate, veratridine, creatine and other substances. Brain Res 1986;378:390–393. [PubMed: 2425906]

Lescot T, Degos V, Puybasset L. Does the brain become heavier or lighter after trauma? Eur J Anaesthesiol Suppl 2008;42:110–114. [PubMed: 18289427]

McElvain JS, Schenk JO. Blockade of dopamine autoreceptors by haloperidol and the apparent dynamics of potassium-stimulated endogenous release of dopamine from and reuptake into striatal suspensions in the rat. Neuropharmacology 1992;31:649–659. [PubMed: 1407404]

Motulsky, HJ.; Christopoulos, A. Fitting Models to Biological Data Using Linear and Non-linear Regression: A Practical Guide to Curve Fitting. Vol. 2nd ed.. San Diego: GraphPad Software, Inc.;

Patrick KS, Ellington KR, Breese GR. Distribution of methylphenidate and phydroxymethylphenidate in rats. J Pharmacol Exp Ther 1984;231:61–65. [PubMed: 6491975]

Riddle EL, Hanson GR, Fleckenstein AE. Therapeutic doses of amphetamine and methylphenidate selectively redistribute the vesicular monoamine transporter-2. Eur. J. Pharmacol 2007;571:25–28. [PubMed: 17618619]

Riddle EL, Topham MK, Haycock JW, Hanson GR, Fleckenstein AE. Differential trafficking of the vesicular monoamine transporter-2 by methamphetamine and cocaine. Eur. J. Pharmacol 2002;449:71–74. [PubMed: 12163108]

Sabatini U, Celsis P, Viallard G, Rascol A, Marc-Vergnes JP. Quantitative assessment of cerebral blood volume by single-photon emission computed tomography. Stroke 1991;22:324–330. [PubMed: 1848374]

Sandoval V, Riddle EL, Hanson GR, Fleckenstein AE. Methylphenidate redistributes vesicular monoamine transporter-2: Role of dopamine receptors. J. Neurosci 2002;22:8705–8710. [PubMed: 12351745]

Sandoval V, Riddle EL, Ugarte YV, Hanson GR, Fleckenstein AE. Methamphetamine-induced rapid and reversible changes in dopamine transporter function: an in vitro model. J. Neurosci 2001;21:1413–1419. [PubMed: 11160413]

Schenk JO, Wright C, Bjorklund N. Unraveling neuronal dopamine transporter mechanisms with rotating disk electrode voltammetry. J. Neurosci. Methods 2005;143:41–47. [PubMed: 15763135]

Segel, IH. Enzyme Kinetics: Behavior and Analysis of Rapid Equilibrium and Steady-State Enzyme Systems. New York: John Wiley and Sons, Inc.; 1993. p. 18-99.

Thai DL, Yurasits LN, Rudolph GR, Perel JM. Comparative pharmacokinetics and tissue distribution of the d-enantiomers of para-substituted methylphenidate analogs. Drug Metab Dispos 1999;27:645–650. [PubMed: 10348792]

Truong JG, Newman AH, Hanson GR, Fleckenstein AE. Dopamine D2 receptor activation increases vesicular dopamine uptake and redistributes vesicular monoamine transporter-2 protein. Eur. J. Pharmacol 2004;504:27–32. [PubMed: 15507217]

Volz TJ, Bjorklund NL, Schenk JO. Methylphenidate analogs with behavioral differences interact differently with arginine residues on the dopamine transporter in rat striatum. Synapse 2005;57:175–178. [PubMed: 15945061]

Volz TJ, Farnsworth SJ, King JL, Riddle EL, Hanson GR, Fleckenstein AE. Methylphenidate administration alters vesicular monoamine transporter-2 function in cytoplasmic and membraneassociated vesicles. J. Pharmacol. Exp. Ther 2007;323:738–745. [PubMed: 17693585]

Volz TJ, Farnsworth SJ, Rowley SD, Hanson GR, Fleckenstein AE. Methylphenidate-induced increases in vesicular dopamine sequestration and dopamine release in the striatum: the role of muscarinic and dopamine D2 receptors. J Pharmacol Exp Ther 2008;327:161–167. [PubMed: 18591219]

Volz TJ, Hanson GR, Fleckenstein AE. Measurement of kinetically resolved vesicular dopamine uptake and efflux using rotating disk electrode voltammetry. J. Neurosci. Methods 2006;155:109–115. [PubMed: 16480775]

Volz TJ, Schenk JO. A comprehensive atlas of the topography of functional groups of the dopamine transporter. Synapse 2005;58:72–94. [PubMed: 16088952]

Wayment HK, Deutsch H, Schweri MM, Schenk JO. Effects of methylphenidate analogues on phenethylamine substrates for the striatal dopamine transporter: potential as amphetamine antagonists? J. Neurochem 1999;72:1266–1274. [PubMed: 10037500]

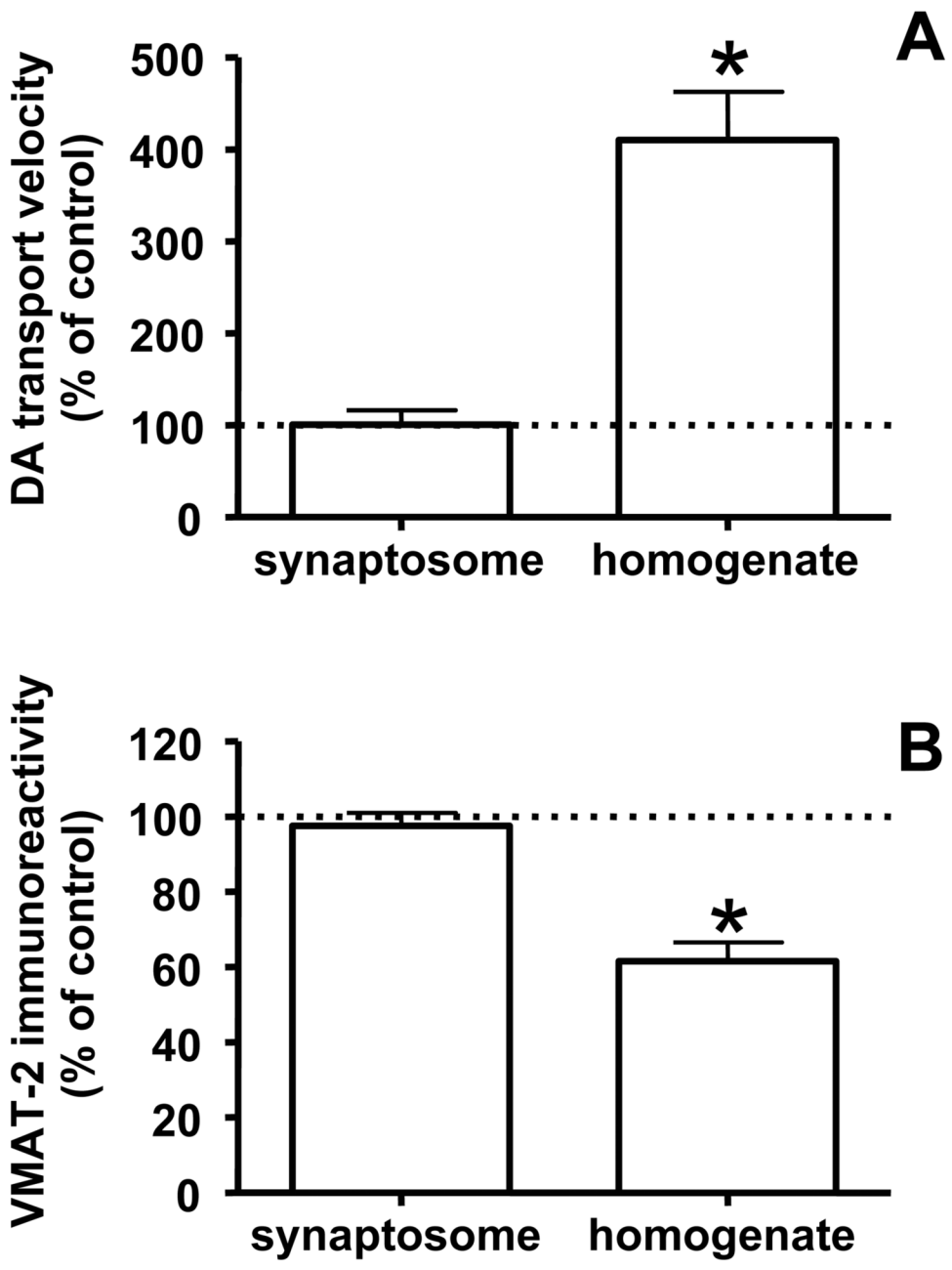

Fig. 1.

In vitro incubation of striatal homogenates, but not striatal synaptosomes, with MPD increases DA transport velocities (Panel A) and decreases VMAT-2 immunoreactivity (Panel B) in membrane-associated vesicles. Striatal homogenates and synaptosomes were incubated with 60 mM MPD for 30 min at 37 °C and then the membrane-associated vesicles were isolated, assayed, and compared with control samples incubated in the absence of MPD. Each column represents the mean ± SEM of four separate measurements. An asterisk indicates a statistical difference, $p < 0.05$ via a paired two-tailed *t*-test, in DA transport velocities or VMAT-2 immunoreactivity in membrane-associated vesicles isolated from striatal homogenates compared to synaptosomes.

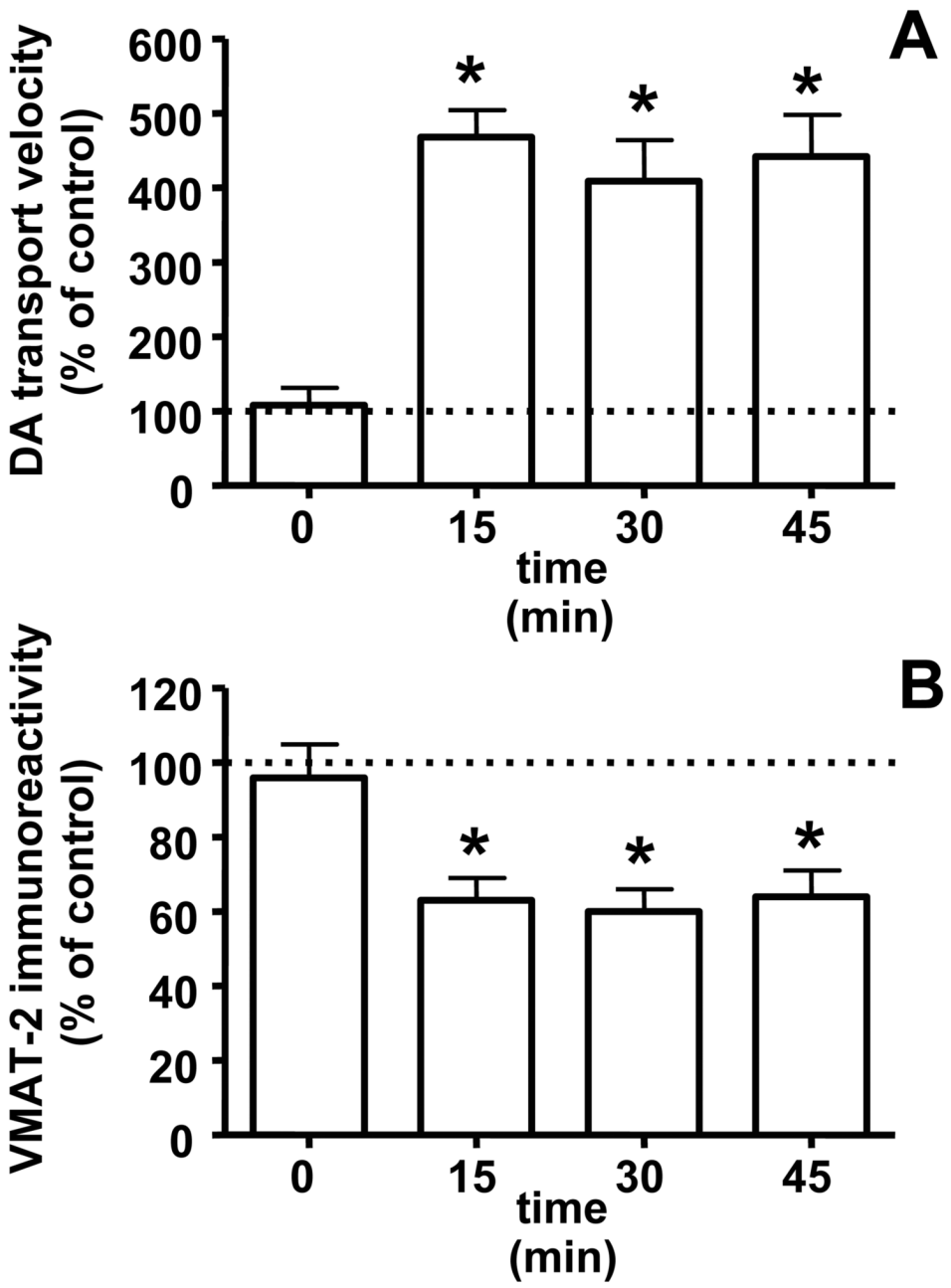

Fig. 2.

In vitro incubation of striatal homogenates with MPD for various times increases DA transport velocities (Panel A) and decreases VMAT-2 immunoreactivity (Panel B) in membraneassociated vesicles. Striatal homogenates were incubated with 60 mM MPD for 0, 15, 30, or 45 min at 37 °C and then the membrane-associated vesicles were isolated, assayed, and compared with control samples incubated in the absence of MPD. Each column represents the mean ± SEM of four separate measurements. An asterisk indicates a statistical difference, $p < 0.05$ via a one-way ANOVA with a Tukey post test, compared to 0 min.

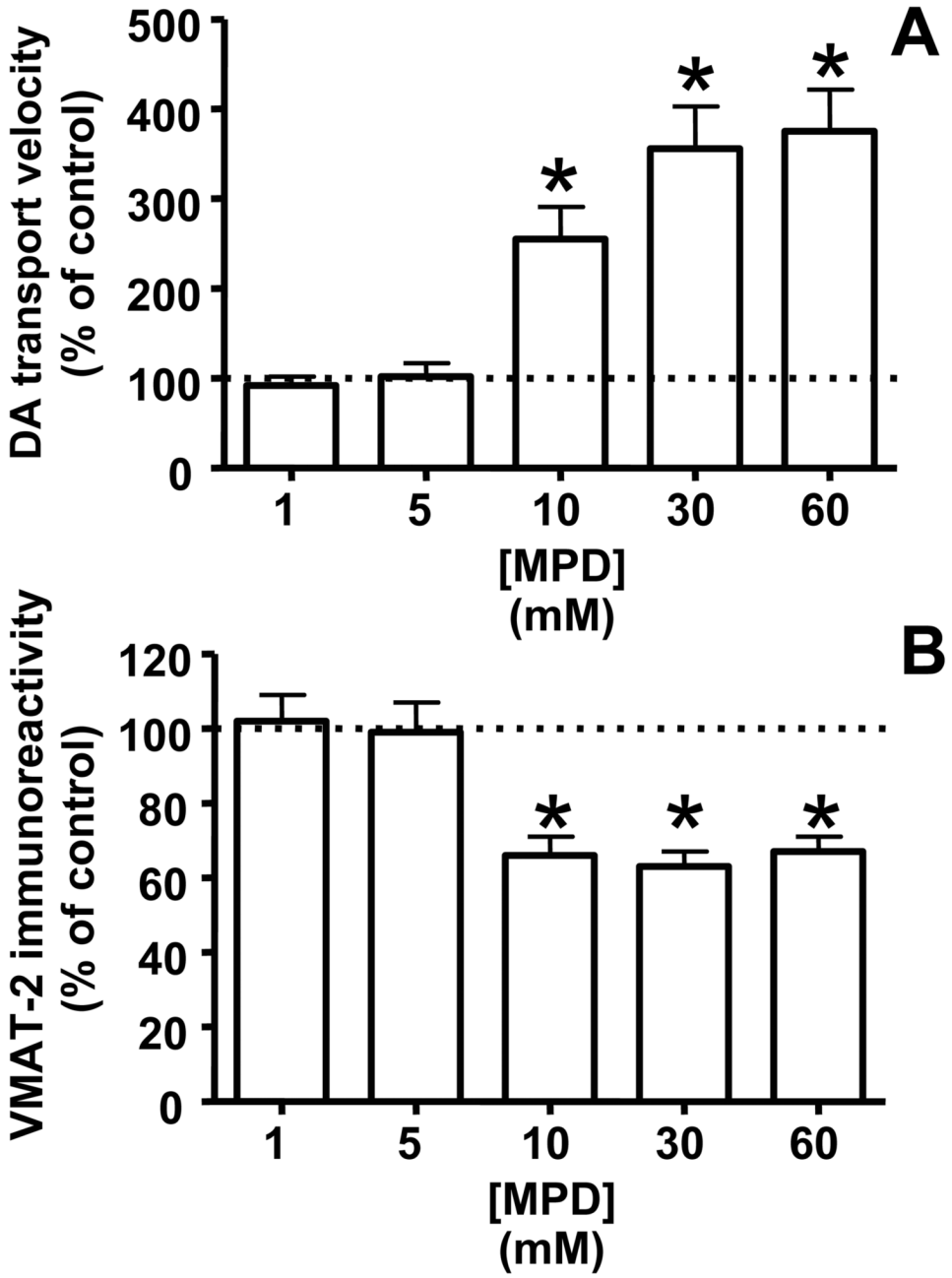

Fig. 3.

In vitro incubation of striatal homogenates with various concentrations of MPD increases DA transport velocities (Panel A) and decreases VMAT-2 immunoreactivity (Panel B) in membrane-associated vesicles. Striatal homogenates were incubated with various concentrations (1–60 mM) of MPD for 30 min at 37 °C and then the membrane-associated vesicles were isolated, assayed, and compared with control samples incubated in the absence of MPD. Each column represents the mean ± SEM of four separate measurements. An asterisk indicates a statistical difference, $p < 0.05$ via a one-way ANOVA with a Tukey post test, compared to 1 or 5 mM MPD.

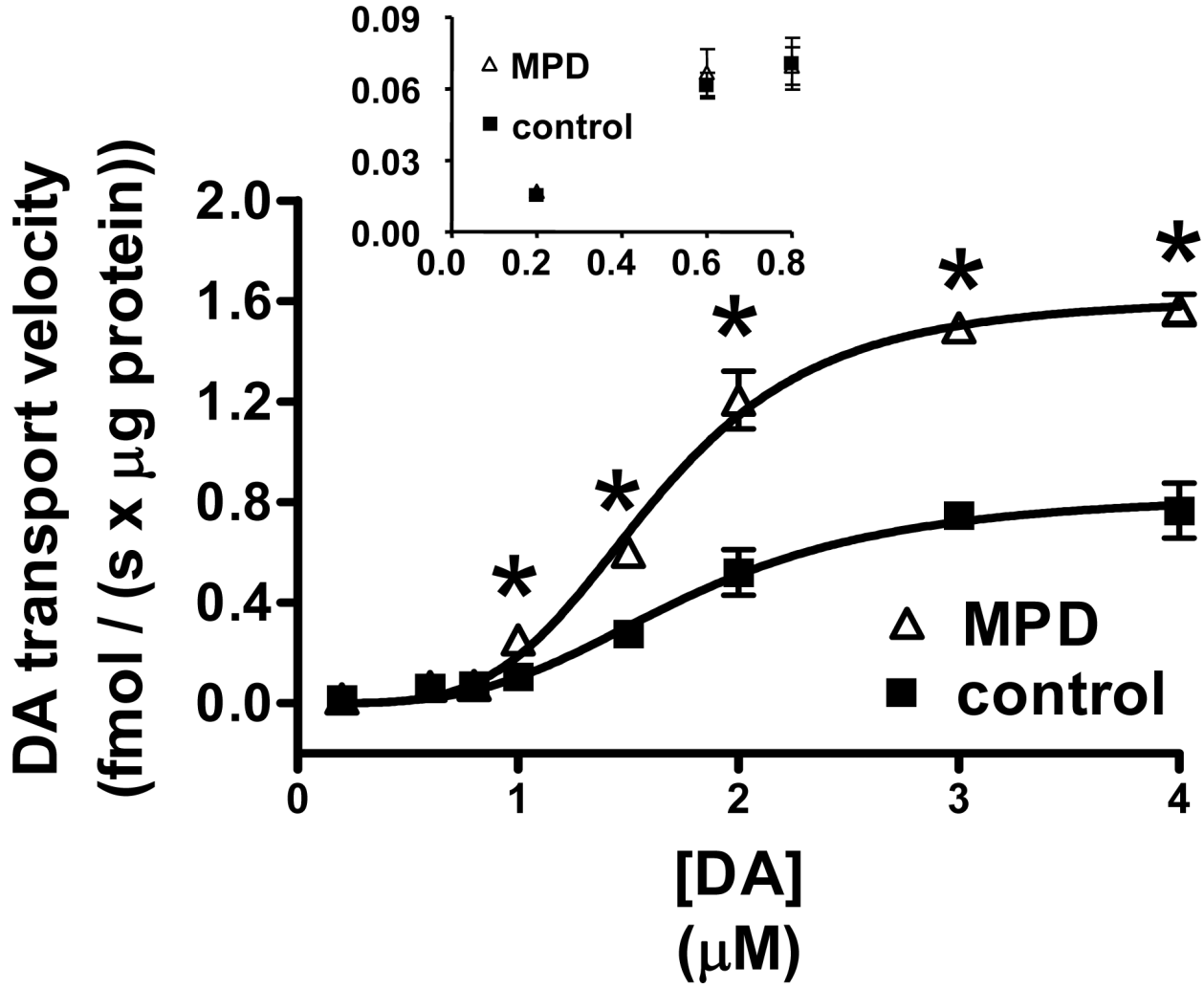

Fig. 4.

DA transport displays non-Michaelis-Menten cooperativity in membrane-associated vesicles isolated from striatal homogenates after *in vitro* incubation. Striatal homogenates were incubated either in the absence of MPD (control) or with 10 mM MPD (MPD) for 30 min at 37 °C and then the membrane-associated vesicles were isolated and assayed. Each datum point represents the mean ± SEM of four separate measurements and an asterisk indicates a statistical difference, $p < 0.05$ via a paired two-tailed *t*-test, compared to control. The solid lines represent the best fits of the Hill equation (Eq. 1) to the observed data with r^2 values of 0.9821 (control) and 0.9759 (MPD). DA transport velocities at the lowest concentrations of DA are magnified in the inset.

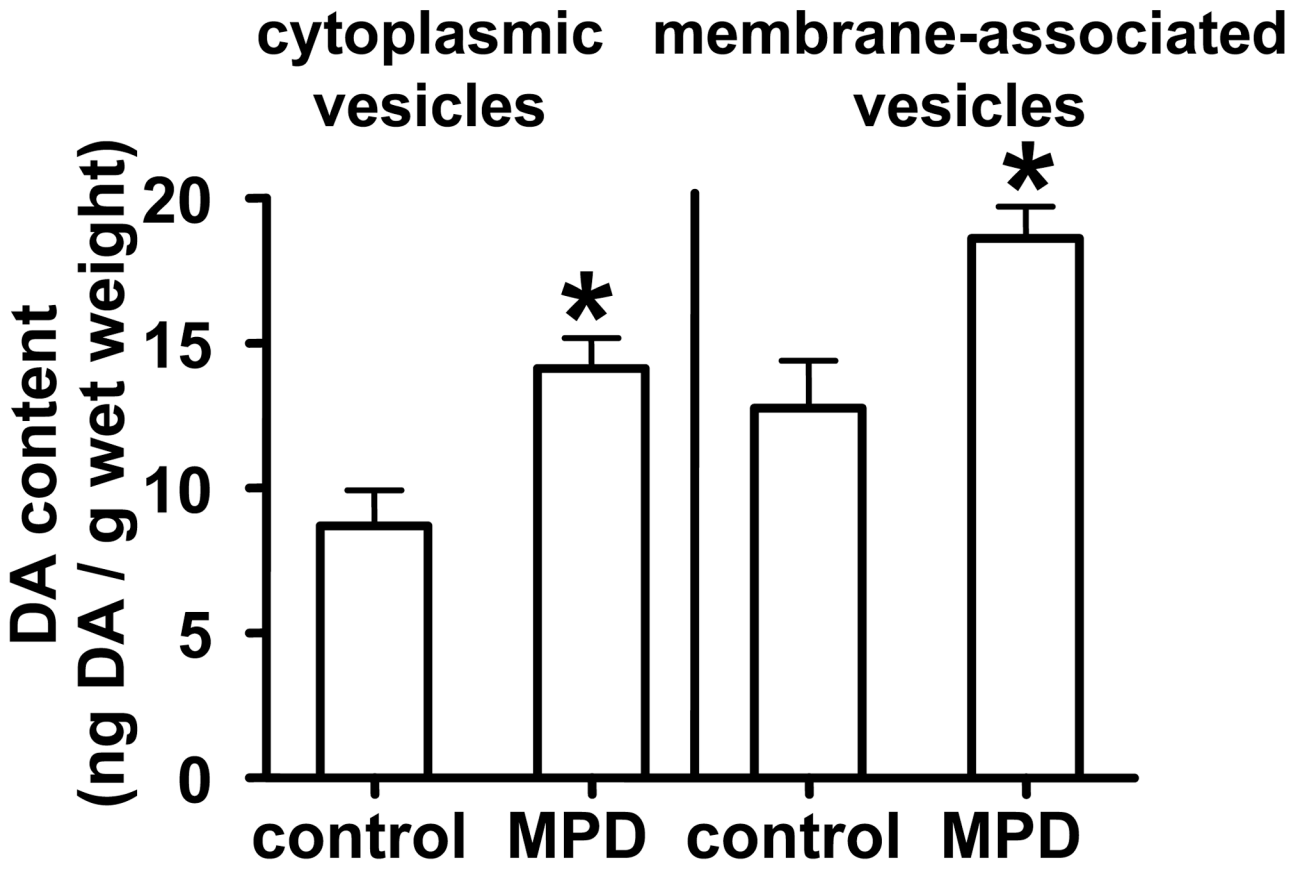

Fig. 5.

In vitro incubation of striatal homogenates with MPD increases DA content in both cytoplasmic and membrane-associated vesicles. Striatal homogenates were incubated either in the absence of MPD (control) or with 10 mM MPD (MPD) for 30 min at 37 °C and then the vesicles were isolated and assayed. Each column represents the mean ± SEM of six separate measurements. An asterisk indicates a statistical difference, $p < 0.05$ via a paired two-tailed *t*-test, between control and MPD.

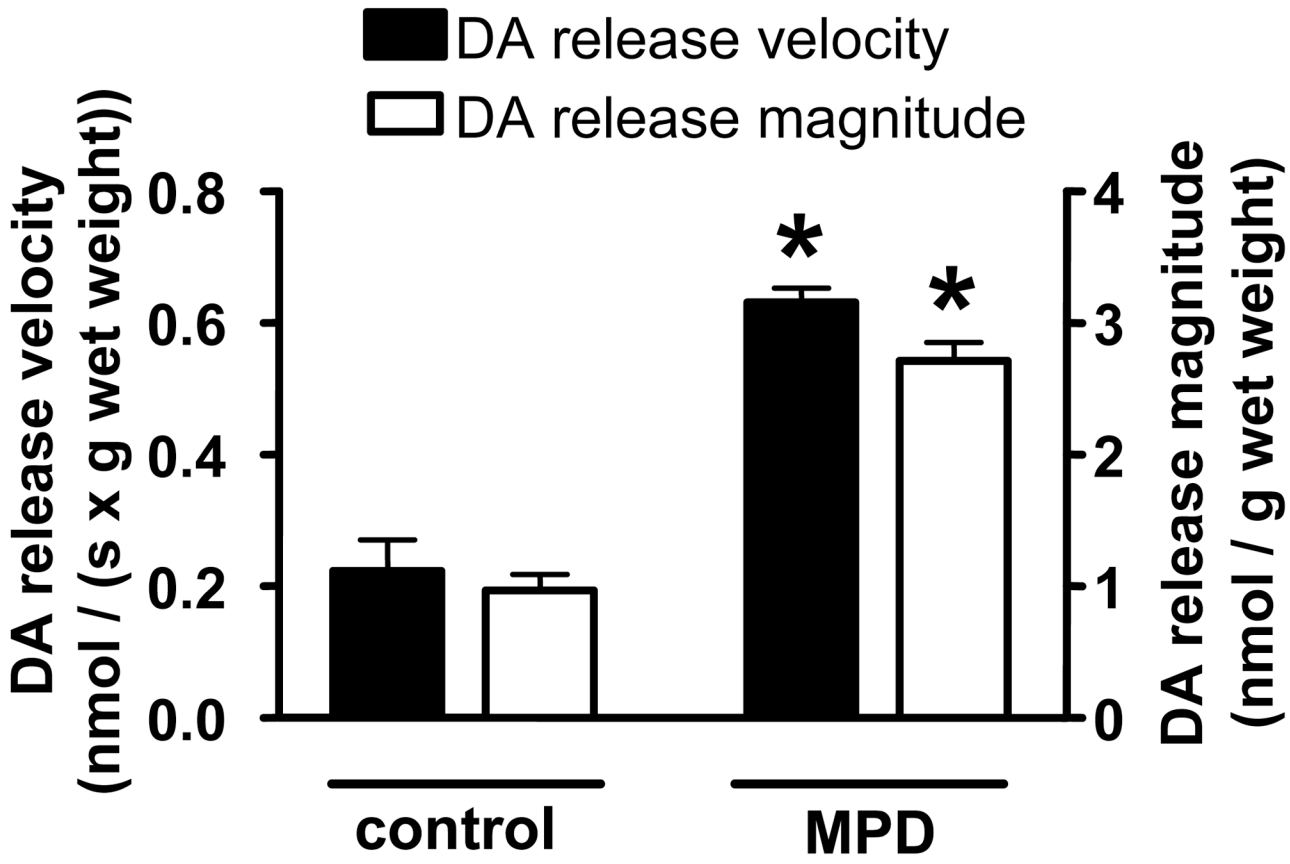

Fig. 6.

In vitro incubation of striatal homogenates with MPD increases both the magnitude and velocity of K^+-stimulated DA release. Striatal homogenates were incubated either in the absence of MPD (control) or with 10 mM MPD (MPD) for 30 min at 37 °C and then assayed. Each column represents the mean ± SEM of four separate measurements. An asterisk indicates a statistical difference, $p < 0.05$ via a paired two-tailed *t*-test, between control and MPD.